SURE 静岡大学学術リポジトリ
Shizuoka University REpository

Development of Rous sarcoma Virus-like Particles Displaying hCC49 scFv for Specific Targeted Drug Delivery to Human Colon Carcinoma Cells

メタデータ	言語: eng 出版者: 公開日: 2016-07-06 キーワード (Ja): キーワード (En): 作成者: Kato, Tatsuya, Yui, Megumi, Deo, Vipin Kumar, Park, Enoch Y. メールアドレス: 所属:
URL	http://hdl.handle.net/10297/9722

Development of *Rous sarcoma* Virus-like Particles Displaying hCC49 scFv for Specific Targeted Drug Delivery to Human Colon Carcinoma Cells

Tatsuya Kato・Megumi Yui・Vipin Kumar Deo・Enoch Y. Park*

Running Head: Specific drug delivery to LS174T cells using RSV VLPs

Tatsuya Kato・Megumi Yui・Enoch Y. Park (✉)
Laboratory of Biotechnology, Department of Applied Biological Chemistry, Faculty of Agriculture, Shizuoka University, 836 Ohya, Shizuoka 422-8529, Japan
Tel.: +81 54 238 4887; fax: +81 54 238 4887. e-mail: acypark@ipc.shizuoka.ac.jp

Vipin Kumar Deo, Tatsuya Kato, Enoch Y. Park
Graduate School of Science and Technology, Shizuoka University, 836 Ohya, Shizuoka 422-8529, Japan

Tatsuya Kato・Enoch Y. Park
Research Institute of Green Science and Technology, Shizuoka University, 836 Ohya, Suruga-ku, Shizuoka 422-8529, Japan

ABSTRACT

Purpose: Virus-like particles (VLPs) have been used as drug carriers for drug delivery systems. In this study, hCC49 single chain fragment variable (scFv)-displaying *Rous sarcoma* virus-like particles (RSV VLPs) were produced in silkworm larvae to be a specific carrier of an anti-cancer drug.

Method: RSV VLPs displaying hCC49 scFv were created by the fusion of the transmembrane and cytoplasmic domains of hemagglutinin from influenza A (H1N1) virus and produced in silkworm larvae. The display of hCC49 scFv on the surface of RSV VLPs was confirmed by enzyme-linked immunosorbent assay using tumor-associated glycoprotein-72 (TAG-72), fluorescent microscopy, and immunoelectron microscopy. Fluorescein isothiocyanate (FITC) or doxorubicin (DOX) was incorporated into hCC49 scFv-displaying RSV VLPs by electroporation and specific targeting of these VLPs was investigated by fluorescent microscopy and cytotoxicity assay using LS174T cells.

Results: FITC was delivered to LS174T human colon adenocarcinoma cells by hCC49 scFv-displaying RSV VLPs, but not by RSV VLPs. This indicated that hCC49 scFv allowed FITC-loaded RSV VLPs to be delivered to LS174T cells. DOX, which is an anti-cancer drug with intrinsic red fluorescence, was also loaded into hCC49 scFv-displaying RSV VLPs by electroporation; the DOX-loaded hCC49 scFv-displaying RSV VLPs killed LS174T cells via the specific delivery of DOX that was mediated by hCC49 scFv. HEK293 cells were alive even though in the presence of DOX-loaded hCC49 scFv-displaying RSV VLPs.

Conclusion: These results showed that hCC49 scFv-displaying RSV VLPs from silkworm larvae offered specific drug delivery to colon carcinoma cells in vitro. This scFv-displaying enveloped VLP system could be applied to drug and gene delivery to

other target cells.

KEY WORDS: drug delivery・colon carcinoma・*Rous sarcoma* virus-like particles・silkworm・doxorubicin

ABBREVIATIONS

CLSM	confocal laser scanning microscope
BmNPV	*Bombyx mori* nucleopolyhedrovirus
BmNPV/RSV-gag-577	BmNPV bacmid encoding the RSV gag protein gene
BSA	Bovine serum albumin
DOX	doxorubicin
DLS	dynamic light scattering
ELISA	enzyme-linked immunosorbent assay
FITC	fluorescein isothiocyanate
gag	group antigen protein
GPI	glycosylphosphatidylinositol
HA	hemagglutinin
hCC49	humanized CC49 antibody
HRP	horseradish peroxidase
MTT	3-(4,5-di-methylthiazol-2-2yl)-2,5-diphenyltetrazolium bromide
PBS	phosphate-buffered saline
RSV	*Rous sarcoma* virus
RSV VLPs	*Rous sarcoma* virus-like particles
scFv	single-chain variable fragment
TAG-72	tumor associated glycoparticle-72
VLPs	virus-like particles

INTRODUCTION

Virus-like particles (VLPs) derived from various viruses have been utilized for vaccines, as well as gene and drug delivery systems. VLPs have nearly the same properties as intact viruses, but they have no genomic DNA or RNA that encodes viral proteins. Therefore, safety concerns related to the use of inactivated or attenuated viruses can be mitigated, especially for in vivo applications of VLPs. Additionally, VLPs have empty interior space in which various materials, drugs, nucleic acids, and nanoparticles can be loaded for gene and drug delivery (1, 2). Non-enveloped VLPs can be produced through the expression of a viral capsid protein. Expressed capsids are self-assembled and form VLPs. These VLPs sometimes have nucleic acids derived from host cells, but the nucleic acids can be removed by the disassembly of VLPs. The disassembly and reassembly of VLPs ensures a uniform size of VLPs (3). Enveloped VLPs have a lipid membrane and an envelope that are derived from host cells when the VLPs self-assemble and bud from host cells. When enveloped VLPs are expressed simultaneously with membrane proteins, the membrane proteins are embedded into the envelope of VLPs during the budding process (2).

VLPs can be functionalized through various methods to provide specificity as nanoparticles. The surface and the interior of VLPs can be specialized for functions including cell specificity, display of immunological antigens, and stabilization by chemical and genetic modification. The surface of non-enveloped VLPs can be functionalized by a covalent approach through amino acid residues on the surface, including lysine, cysteine, and others (4). This covalent modification is an irreversible reaction, which is favorable for long-term binding to targets. Alternatively, peptides and proteins can be displayed on the surface of non-enveloped VLPs by using a fusion technique with virus capsid proteins. Enveloped VLPs can also be functionalized chemically and genetically through the modification of envelope proteins. The fusion of a foreign protein with a full-length or transmembrane domain of a viral envelope protein enables

its protein to be displayed on the surface of enveloped VLPs (5, 6). Additionally, foreign transmembrane proteins can be displayed on enveloped VLPs by their co-expression in hosts, which allows for multifunctional VLPs (1, 7).

Recently, *Rous sarcoma* virus (RSV) VLPs displaying a scFv of humanized CC49 antibody (hCC49) were produced in silkworm larvae in order to target the specific delivery of drugs to colon carcinoma cells (8). In this case, hCC49 scFv was linked by glycosylphosphatidylinositol (GPI) anchor on the surface of RSV VLPs. These particles specifically delivered sulforhodamine B to colon carcinoma cells, LS174T cells. In other paper, using RSV gag protein and M1 protein from influenza A virus, chimeric VLPs were produced in silkworm larvae and applied to drug delivery system and vaccine production (9). Modification of RSV VLPs can provide these particles various capacities.

In this study, RSV VLPs displaying hCC49 scFv by using transmembrane and cytoplasmic domains of hemmaglutinin (HA) from influenza A virus were produced in silkworm larvae for the application to drug delivery system, instead of the use of GPI anchor reported previously (8). The hCC49 scFv binds specifically to tumor-associated glycoprotein-72 (TAG-72) on the surface of colon carcinoma cells (10, 11). TAG-72 is also expressed very low level in human adenocarcinomas of the colon, pancreas, and breast, but it is not expressed in normal tissues (12). Doxorubicin (DOX) was used as an anti-cancer drug to be delivered to colon carcinoma cells by hCC49 scFv-displaying RSV VLPs.

MATERIALS AND METHODS

Cell Lines, Media, and Silkworms

LS174T human colon adenocarcinoma (ATCC CL-188) and HEK293 (RCB1637) cell lines were purchased from ATCC (Manassas, VA, USA) and Riken Bio Resource Center (Tsukuba,

Ibaraki, Japan), respectively. LS174T cells were cultured in 25-cm^2 T-flasks with MEM-Eagle medium (Sigma-Aldrich, St. Louis, MO, USA) containing 10% (v/v) fetal bovine serum (Invitrogen, Carlsbad, CA, USA) and supplemented with 1% (v/v) antibiotic solution containing penicillin, streptomycin, and fungizone (Sigma-Aldrich). The cultures were placed in an incubator (MCO-175 Sanyo, Osaka, Japan) maintained at 37°C with 5% CO_2. HEK293 cells were cultured in 25-cm^2 T-flasks with MEM/EBSS medium (HyClone Laboratories Inc., Utah, USA) containing 2 mM L-glutamine, 1% non-essential amino acid solution (Invitrogen), and 10% fetal bovine serum and supplemented with 1% (v/v) antibiotic solution containing penicillin, streptomycin, and fungizone. The cultures were placed in an incubator maintained at 37°C with 5% CO_2.

Molting fourth instars of silkworm larvae were purchased from Ehimesansyu (Yahatahama, Ehime, Japan). Silkworm larvae were reared on an artificial diet of Silkmate 2S (Nihon Nosan Kogyo, Yokohama, Japan) in a 60% humidity chamber (MLR-351H, Sanyo, Tokyo, Japan) maintained at 25°C.

Construction of Recombinant Bacmids

The construction of the *Bombyx mori* nucleopolyhedrovirus (BmNPV) bacmid for the expression of the RSV gag protein (BmNPV/RSV-gag-577) was described previously (13). The scFv of hCC49 was amplified by PCR using Eco-bx-FLAG-hCC49scFv and scFv-spe primers (Table 1) with pROX-FL92amber (hCC49) (kindly donated by Professor Hiroshi Ueda, Tokyo Institute of Technology) as a template. Also, the C-terminal domain of HA was amplified by PCR using Spe-H1N1 and H1N1-Hind primers (Table 1) with Influenza A (H1N1, A/New Caledonia/20/99) HA cDNA clone (Sino Biological Inc., Beijing, China) as a template. The scFv fragments were digested by *Eco*RI and *Spe*I, and the C-terminal domain of HA was digested by *Spe*I and *Hin*dIII. The digested fragments were ligated into the *Eco*RI – *Hin*dIII

site in the pFastBac1 vector. The constructed vector was transformed into *E. coli* BmDH10Bac (14). The recombinant BmNPV (BmNPV/hCC49-scFv) bacmid was extracted from a white transformant.

Production and Purification of RSV VLPs in Silkworm Larvae

Each recombinant BmNPV bacmid was mixed in a 1:1 ratio with a total of 10 μg DNA. The bacmid mixture was then mixed with 1/10 volume of DMRIE-C reagent (Life Technologies Japan, Tokyo, Japan) and incubated at room temperature for 30 min. This mixture was injected into the fifth instars of silkworm larvae and these larvae were reared for 6 to 7 days. Hemolymph was collected from bacmid-injected larvae and 1-phenyl-2-thiourea (5 mM) was added to the collected hemolymph. The hemolymph was diluted with phosphate-buffered saline (PBS, pH 7.4) and loaded onto a 25% sucrose cushion; it then was centrifuged to collect VLPs. Pelleted VLPs were suspended with PBS by brief sonication. Sucrose density gradient centrifugation (25–60%) was performed to obtain the VLPs. The top (0.5 ml) fraction was collected from each sample; a total of 10 fractions were collected. These fractions containing VLPs were dialyzed with PBS using a dialysis membrane with a molecular weight cutoff of 300 kDa (Spectrum Japan, Shiga, Japan).

Protein Concentration Measurement and Western Blot

Protein concentration was measured using the Reducing Agent Compatible version of the BCA Protein Assay (Thermo Fisher Scientific, Rockford, IL, USA). SDS-PAGE and western blot were conducted as described in previous papers (13). For the western blot, mouse anti-FLAG M2 antibody (Sigma-Aldrich) or mouse anti-DYKDDDDK tag antibody (Wako Pure Chemical Industries, Osaka, Japan) was used as the primary antibody to detect hCC49 scFv. Sheep anti-mouse IgG antibody (GE healthcare Japan, Tokyo, Japan) was also used as a secondary

antibody.

Enzyme-linked Immunosorbent Assay

For the enzyme-linked immunosorbent assay (ELISA), TAG-72 antigen from human fluids (Sigma-Aldrich) diluted to 10 U/ml with PBS was loaded into each well of a 96-well plate. Bovine serum albumin (BSA) dissolved with PBS to a final concentration of 10 μg/ml was used as a negative control. The plates were blocked with 2% skimmed milk dissolved with PBS at room temperature for 2 h. Each well was washed three times with PBS and then samples diluted with 2% skimmed milk were added into each well; the plate was then incubated at room temperature for 1 h. Each well was washed three times with PBS and then horseradish peroxidase (HRP)-conjugated anti-FLAG M2 antibody (Sigma-Aldrich) diluted 5000-fold with 2% skimmed milk was added. The plate was incubated at room temperature for 1 h and washed with PBS. Then, the HRP reaction was performed to measure absorbance at 450 nm in each well.

Immunogold-labeling in Transmission Electron Microscopy and Dynamic Light scattering (DLS) measurement

The hCC49 scFv-displaying RSV VLPs were placed on carbon grids (Okenshoji, Tokyo, Japan) and dried at room temperature. The grids were blocked with 4% BSA for 1 h and washed with PBS. The grids were incubated with 100 fold-diluted mouse anti-DYKDDDDK monoclonal antibody (Wako) for 2 h and then washed with PBS. The grids were then incubated with 200-fold diluted goat polyclonal anti-mouse IgG+IgM (H+L) conjugated with 10-nm gold particles (BB International, Cardiff, UK) for 2 h and washed with PBS. Negative staining was performed using 2% phosphotungstic acid and VLPs were observed using a transmission electron microscope (JEM2100F-TEM, JEOL, Tokyo, Japan).

For DLS measurement, the samples were loaded onto disposable cuvettes (DTS-1061) for the measurement of size with the Zetasizer Nano series (Malvern, Worcestershire, United Kingdom).

Loading Fluorescein isothiocyanate (FITC) and DOX into RSV VLPs

FITC, a fluorescent material, and DOX, an anti-cancer drug, were used as loading compounds. To load these materials into RSV VLPs, 100 μg/ml FITC or 50 μg/ml DOX were mixed with 0.5 mg of protein/ml RSV VLPs and this mixture was electroporated using the Gene Pulser Xcell system (BIO-RAD, Hercules, CA, USA) (250 V, 750 μF). After electroporation, the mixture was cooled on ice, dialyzed, and concentrated with Amicon Ultra centrifugal filters with a membrane nominal molecular weight limit of 30 kDa (Merck Millipore, Billerica, MA, USA).

Fluorescence Microscopy

For immunofluorescence microscopy, 2000 cells of human LS174T and HEK293 cell lines were seeded onto a slide glass coated with polylysine. Cells were fixed with 10% formaldehyde for 20 min. The slide glass was washed four times with PBS and the remaining formaldehyde was removed using 50 mM NH_4Cl. The slide glass was again washed four times with PBS and then the slide glass was blocked with 4% BSA at room temperature for 2 h. The slide glass was washed four times with PBS and then VLPs were added to cells on the slide glass and incubated at room temperature for 2 h. The slide glass was washed four times with PBS and then incubated with 5000-fold diluted mouse anti-DYKDDDDK tag monoclonal antibody (Wako) at room temperature for 1 h. The slide glass was washed four times and then 1000-fold diluted goat polyclonal anti-mouse IgG (H & L) conjugated with Alexa597 (Abcam, Tokyo, Japan) was added to the cells; the slide glass was incubated at room temperature for 1 h. Finally, the

slide glass was washed four times with PBS and the cells were observed using a confocal laser scanning microscope (CLSM) (LSM 700, Carl Zeiss, Oberkochen, Germany).

For the analysis of chemical delivery, 2000 cells of human LS174T and HEK293 cell lines were seeded onto an aminosilane-coated slide glass with chambers and cultivated at 37°C for 24 h. Culture media in each chamber was discarded and VLP solution was added into each chamber. The slide glass was incubated at 37°C for 24 h and the cells were fixed with 10% formaldehyde for 20 min. The slide glass was washed three times and the remaining formaldehyde was removed with 50 mM NH_4Cl. Finally, 4'6-diamidino-2-phenylindole was added to the cells and the stained cells were observed using CLSM.

3-(4,5-di-Methylthiazol-2-2yl)-2,5-Diphenyltetrazolium Bromide (MTT) Assay

2000 cells of human LS174T and HEK293 cell lines were seeded into each well of a 96-well plate and cultivated at 37°C for 48 h. Culture medium was replaced with fresh medium and 10 μl of 0.2 mg of protein/ml VLP were added into each well. After 24 h of cultivation, the MTT assay was conducted using the MTT Cell Proliferation/Viability Assay Kit (Trevigen, Gaithersburg, MD, USA). Viability was calculated by the following formula:

$$\text{Cell viability (\%)} = \frac{(A_s - A_b)}{(A_c - A_b)} \times 100$$

where A_s, A_b, and A_c denote absorbances of sample, blank, and negative control (cell only).

RESULTS

Co-expression of RSV gag Proteins and hCC49 scFv in Silkworm Larvae

RSV gag protein was expressed in silkworm larvae and formed successfully enveloped VLPs in the hemolymph of silkworm larvae (13). The hCC49 scFv was displayed on the surface of

RSV VLPs that specifically targeted colon adenocarcinoma cells. To display this scFv on the VLPs, the C-terminal domain of HA from Influenza A (H1N1), which contains its transmembrane and cytoplasmic domains, was fused at the C-terminus of scFv (Fig. 1). The recombinant BmNPV bacmid harboring these genes under the polyhedrin promoter was constructed. Using BmNPV/RSV-gag-577 and BmNPV/hCC49-scFv bacmids, the gag protein of RSV and hCC49 scFv were co-expressed in silkworm larvae. The gag protein of RSV has been expressed and processed in various forms (13, 15). Most of the RSV gag protein and hCC49 scFv were expressed in the fat body of silkworm larvae (Fig. 2A). After sucrose density gradient centrifugation, RSV gag protein and hCC49 scFv were observed in the purified sample (Fig. 2B).

Characterization of hCC49 scFv-displaying RSV VLPs

To confirm the display of hCC49 scFv on the surface of these VLPs, ELISA, immunoelectron microscopy, and immunofluorescence microscopy were performed using LS174T cells. Incubation of purified hCC49 scFv-displaying RSV VLPs with LS174T cells yielded specific fluorescence around the cells (upper panel of Fig. 3A). However, purified RSV VLPs to LS174 cells did not provided red fluorescence around LS174T cells (lower panel of Fig. 3A). It indicated that hCC49scFv allowed RSV VLPs to bind specifically to TAG-72 on the surface of LS174T cells. The TAG-72 expression was confirmed by western blot (Supplementary Figure 1). In addition, ELISA revealed specific binding of these purified VLPs to TAG-72; the purified VLPs were compared to a negative control using BSA (Fig. 3B). Gold particles were observed on the surface of purified RSV VLPs (Fig. 3C). The average diameters of RSV VLPs and hCC49 scFv-displaying RSV VLPs were approximately 50 nm and 90 nm, respectively (Fig. 3D). These results indicated that hCC49 scFv was displayed on the surface of hCC49 scFv-displaying RSV VLPs.

Fluorescent Compound Loading and Delivery

FITC was loaded into hCC49 scFv-displaying RSV VLPs and used to model delivery to target cells. FITC was loaded into VLPs by electroporation. LS174T cells treated with FITC-loaded hCC49 scFv-displaying RSV VLPs were observed using CLSM and green fluorescence of FITC was observed inside the cells (Fig. 4). However, only slight green fluorescence of FITC was observed in LS174T cells treated with FITC-loaded RSV VLPs. This indicated that the hCC49 scFv allowed RSV VLPs to specifically target LS174T cells and FITC was specifically delivered to these cells.

To further investigate the possibility to use hCC49 scFv-displaying RSV VLPs for drug delivery system, DOX-loaded hCC49 scFv-displaying RSV VLPs was prepared. DOX was used as a model of an anti-cancer drug in this study. DOX causes intercalation of DNA in cancer cells, which leads to cancer cell death, but DOX has several adverse effects, including serious heart damage. Specific delivery of DOX to target cells would reduce its adverse effects. DOX can be easily measured by either fluorescent microscope or fluorescence spectrophotometer because it exhibits red fluorescence (ex. 480 nm, em. 575 nm). Approximately 14 μg/ml of DOX (10 μl) was loaded in 200 μg of protein of hCC49 scFv-displaying RSV VLPs by electroporation (incorporation efficiency 0.7%, data not shown). LS174T cells were treated with DOX-loaded hCC49 scFv-displaying RSV VLPs and DOX-loaded RSV VLPs. DOX-loaded RSV VLPs were used as a control. The cytotoxicity of these VLPs was investigated using LS174T cells and HEK293 cells. The viability of LST174T cells treated with DOX-loaded hCC49 scFv-displaying RSV VLPs decreased by 35%, but the viability of HEK293 cells treated with the same VLPs remained at 100% (Fig. 5). This indicated that hCC49 scFv-displaying RSV VLPs specifically recognized LS174T cells and delivered DOX to LS174T cells. Non-specific delivery of DOX to HEK293 cells was not observed. In addition, the cytotoxicity of DOX-loaded RSV VLPs to LS174T cells and HEK293 cells was not observed,

which indicated that hCC49 scFv displayed on the surface of RSV VLPs recognized its antigen, TAG-72, on the surface of LS174T cells. Free DOX (10 μg/ml, total amount 0.1 μg) killed 18% LS174T cells, but DOX-loaded hCC49 scFv-displaying RSV VLPs (amount of DOX loading: 0.14 μg) have the higher cytotoxicity specific to LS174T cells (35%). It indicated that DOX-loaded hCC49 scFv-displaying RSV VLPs was more efficient to kill LS174T cells than free DOX even if the same amount of DOX loaded into hCC49 scFv-displaying RSV VLPs was used as free DOX. In this experiment, it is possible that DOX is adhered to these VLPs on the surface, not loaded inside these VLPs, and delivered to LS174T cells. To exclude this possibility, hCC49 scFv-displaying RSV VLPs, which was purified after just mixing with 50 μg/ml DOX, were used as a control. The hCC49 scFv-displaying RSV VLPs mixed with DOX slightly killed LS174T cells (8%), but DOX-loaded hCC49 scFv-displaying RSV VLPs killed more LS174T cells (35%). This result indicated DOX was not adhered to the surface of hCC49 scFv-displaying RSV VLPs by mixing with free DOX and was loaded to these VLPs by electroporation.

DISCUSSION

In this study, hCC49 scFv-displaying RSV VLPs were produced by the co-expression of RSV gag protein and hCC49 scFv fused with the C-terminal domain of HA in silkworm larvae. Specific delivery of DOX to LS174T cells was completed using these RSV VLPs. When RSV VLPs are prepared using BmNPV bacmid in silkworm larvae, GP64, which is a major baculoviral envelope protein, is displayed on the surface of RSV VLPs (16). GP64 is essential for the transduction of baculoviruses into mammalian cells and is attached to the cell surface and internalized by receptor-mediated endocytosis followed by low pH-triggered membrane fusion (17–19). The interaction of GP64 with phospholipids and cholesterol heparin mediates

baculovirus internalization to mammalian cells (20–22). In this study, hCC49 scFv displayed on the surface of RSV VLPs allowed DOX to be specifically delivered to LS174T cells (Figs. 4 and 5). DOX was not specifically delivered to LS174T cells using RSV VLPs, even though RSV VLPs have GP64 on the surface (Figs. 4 and 5). These results suggest that the specificity of hCC49 scFv to LS174T cells is high, which enables specific delivery of DOX to LS174T cells without its non-specific delivery via GP64. Antibodies can be also conjugated with VLPs and various nanoparticles, but, sometimes, antibodies lose ligand capacity by promiscuous conjugation with VLPs and nanoparticles.

When RSV gag protein was co-expressed with hCC49 scFv fused with the C-terminal region of HA from influenza A virus, no modification steps were needed to obtain hCC49 scFv-displaying RSV VLPs in silkworms. The fusion of hCC49 scFv with the C-terminal domain of HA did not disturb its binding capacity to the antigen and its active scFv on the surface of RSV VLPs specifically bound to colon carcinoma cells, LS174T cells (Fig. 3A and 3B). Antibody-display system on the surface of envelope VLPs using a heterologous transmembrane domain is useful for drug delivery to target cells. This system can be applied to the other expression systems using yeasts, insect cells and mammalian cells instead of silkworms. Especially, monoclonal antibodies against antigens specific to cancer cells have been utilized for drug delivery and tumor cell imaging because of the high specificities to ligands (23). Monoclonal antibodies have the potential to specifically deliver drugs to targeted cells, which could minimize side effects and reduce drug doses. Among monoclonal antibodies, monoclonal scFv, which was also used in this study, is the best choice to be displayed on the surface of nanomaterials including VLPs because of its size and structure.

Several methods of loading drugs into enveloped viruses and VLPs have been reported. Electroporation enables carboxylated quantum dots to be loaded into enveloped VLPs (24). In the case of human hepatitis B virus (HBV) particles composed of L protein, the fusion of HBV

313 particles with liposomes containing DNA is more efficient for loading DNA than
314 electroporation (2, 25). In the case of hemagglutinating virus of Japan (HVJ, Sendai virus),
315 detergent treatment, liposome fusion, and electroporation have been applied for the load of
316 drugs, nucleic acids, and nanoparticles (24, 26, 27). For example, detergent treatment of HVJ
317 with centrifugation for plasmid DNA incorporation provides high loading efficiency
318 (approximately 20%) of plasmid DNA into HVJ (28). The loading efficiency of electroporation
319 was 0.7% in this study, but detergent treatment with centrifugation would also be an efficient
320 method for loading various materials, including DOX, into RSV VLPs. In addition, large
321 unilamellar vesicles (LUV) also help DOX and anti-cancer drugs to be loaded into RSV VLPs
322 efficiently (8, 9). However, the use of LUV has more tedious steps than electroporation and
323 detergent treatment.

324 Specific delivery of FITC and DOX to LS174T cells was shown by its fluorescence inside
325 the cells. However, the behavior of these fluorescent materials inside the cells has been still
326 unclear. Viruses can enter into host cells by endocytosis or membrane fusion (29, 30). VLPs
327 can also enter host cells through the same way as viruses. Behaviors of hCC49 scFv-displaying
328 RSV VLPs in LS174T cells and loaded DOX were not determined yet, but DOX seems to reach
329 to nucleus in LS174T cells because DOX-loaded hCC49 scFv-displaying RSV VLPs killed
330 LS174 cells specifically (Fig. 5). However, we have to analyze the internalization pathway of
331 FITC via hCC49 scFv-displaying RSV VLPs or passive transport through lipid bilayer after its
332 release outside the cells from these VLPs. Various endocytosis inhibitors would give the
333 opportunities to reveal the internalization pathway. Alternatively, programmed release system
334 of drugs in cells can carry and release drugs to specific sites in cells and provide more efficient
335 drug delivery to target cells (31, 32).

336 **CONCLUSION**

In this study, hCC49 scFv-displaying RSV VLPs were prepared in silkworm larvae using the BmNPV bacmid system. The C-terminal domain of HA from influenza A (H1N1) virus enabled hCC49 scFv to be anchored into the envelope of RSV VLPs. FITC or DOX was loaded into hCC49 scFv-displaying RSV VLPs by electroporation. DOX were delivered to colon carcinoma cells (LS174T cells) by hCC49 scFv-displaying RSV VLPs and killed LS174T cells, but delivery of DOX to the LS174T cells using DOX-loaded RSV VLPs did not confirm.

ACKNOWLEDGEMENT

We thank Professor Hiroshi Ueda (Tokyo Institute of Technology, Japan) for the contribution of the plasmid carrying scFv cDNA. This work was supported by Grant-in-Aid for Scientific Research (A) Grant No.22248009 and by Promotion of Nanobio-Technology Research to Support Aging and Welfare Society from the Ministry of Education, Culture, Sports, Science and Technology, Japan. No additional external funding was received for this study.

REFERENCES

1. Lua LHL, Connors NK, Sainsbury F, Chuan YP, Wibowo N, Middelberg APJ. Bioengineering virus-like particles as vaccines. Biotechnol Bioeng. 2014;111(3):425–440.
2. Zeltins A. Construction and characterization of virus-like particles: A review. Mol Biotechnol. 2013;53:92–107.
3. Zhao Q, Allen MJ, Wang Y, Wang B, Wang N, Shi L, Sitrin RD. Disassembly and reassembly improves morphology and thermal stability of human papillomavirus type 16 virus-like particles. Nanomedicine. 2012;8(7):1182–1189.
4. Smith MT, Hawes AK, Bundy BC. Reengineering viruses and virus-like particles though chemical functionalization strategies. Curr Opin Biotechnol. 2013;24(4):620–626.
5. Pan YS, Wei HJ, Chang CC, Lin CH, Wei TS, Wu SC, Chang DK. .Construction and

characterization of insect cell-derived influenza VLP: cell binding, fusion, and EGFP incorporation. J Biomed Biotechnol. 2010;2010:506363.

6. Wei HJ, Chang W, Lin SC, Liu WC, Chang DK, Chong P, Wu SC. Fabrication of influenza virus-like particles using M2 fusion proteins for imaging single viruses and designing vaccines. Vaccine. 2011;29(41):7163–7172.

7. Kim YS, Wielgosz MM, Hargrove P, Kepes S, Gray J, Persons DA, Nienhuis AW. Transduction of human primitive repopulating hematopoietic cells with lentiviral vectors pseudotyped with various envelope proteins. Mol Ther. 2010;18(7):1310–1317.

8. Deo VK, Yui M, Alam J, Yamazaki M, Kato T, Park EY. A model for targeting colon carcinoma cells using single-chain variable fragments anchored on virus-like particles via glycosylphosphatidylinositol anchor. Pharm. Res. 2014;31(8):2166-2177.

9. Deo VK, Kato T, Park EY. Chimeric virus-like particles made using GAG and M1 capsid proteins providing dual drug delivery and vaccine platform. Mol. Pharm. 2015, in press

10. Colcher D, Minelli MF, Roselli M, Muraro R, Simpson-Milenic D, Schlom J. Radioimmunolocalization of human carcinoma xenografts with B72.3 second generation monoclonal antibodies. Cancer Res. 1988;48(16):4597–4603.

11. Divig CR, Scott AM, McDermott K, Fallone PS, Hilton S, Siler K, Carmichael N, Daghighian F, Finn RD, Cohen AM, Schlom J, Larson SM. Clinical comparison of radiolocalization of two monoclonal antibodies (mAbs) against the TAG-72 antigen. Nucl Med Biol. 1994;21(1):9–15.

12. Thor A, Ohuchi N, Szpak CA, Johnston WW, Schlom J. Distribution of oncofetal tumor-associated glycoprotein-72 defined by monoclonal antibody B72.3. Cancer Res. 1986;46(6):3118–3124.

13. Deo VK, Tsuji Y, Yasuda T, Kato T, Sakamoto N, Suzuki H, Park EY. Expression of an RSV-gag virus-like particle in insect cell lines and silkworm larvae. J Virol Methods.

2011;177(2):147–152.

14. Motohashi T, Shimojima T, Fukagawa T, Maenaka K, Park EY. Efficient large-scale production of larvae and pupae of silkworm by *Bombyx mori* nucleopolyhedrosis virus bacmid system. Biochem Biophys Res Commun. 2005;326(2):564–569.
15. Xiang Y, Ridky TW, Krishna NK, Leis J. Altered Rous sarcoma virus Gag polyprotein processing and its effects on particle formation. J Virol. 1997;71:2083–2091.
16. Tsuji Y, Deo VK, Kato T, Park EY. Production of Rous sarcoma virus-like particles displaying human transmembrane protein in silkworm larvae and its application to ligand-receptor binding assay. J Biotechnol. 2011;155:185–192.
17. Boyce FM, Bucher NL. Baculovirus-mediated gene transfer into mammaliam cells. Proc Natl Acad Sci USA. 1996;93:2348–2352.
18. Dong S, Wang M, Qiu Z, Deng F, Vlak JM, Hu Z, Wang H. *Autographa californica* multicapsid nucleopolyhedrovirus efficiently infects Sf9 cells transduces mammalian cells via direct fusion with the plasma membrane at low pH. J Virol. 2010;84:5351–5359.
19. Hefferon KL, Oomens AG, Monsma SA, Finnerty CM, Blissard GW. Host cell receptor binding by baculovirus GP64 and kinetics of virus entry. Virology. 1999;258:455-468.
20. Luz-Madrigal A, Asanov A, Camacho-Zarco AR, Sampieri A, Vaca L. A cholesterol recognition amino acid consensus domain in GP64 fusion protein facilitates anchoring og baculovirus to mammalian cells. J Virol. 2013;87:11849–11907.
21. Tani H, Nishijima M, Ushijima H, Miyamura T, Matsuura Y. Characterization of cell-surface determinants important for baculovirus infection. Virology. 2001;279:343–353.
22. Wu S, Wang S. A pH-sensitive heparin-binding sequence from gp64 protein of baculovirus is important for binding to mammalian cells but not to Sf9 cells. J Virol. 2012;86:484–491.
23. Fay F, Scott CJ. Antibody-targeted nanoparticles for cancer therapy. Immunotherapy. 2011;3:381–394.

410 24. Shimbo T, Kawachi M, Saga K, Fujita H, Yamazaki T, Tamai K, Kaneda Y. Development
411 of a transferrin receptor-targeting HVJ-E vector. Biochim Biophys Res Commun.
412 2007;364:423–428.
413 25. Oess S, Hildt E. Novel cell permeable motif derived from the PreS2-domain of hepatitis-B
414 virus surface antigens. Gene Ther. 2000;7:750–758.
415 26. Kaneda Y. Virosome: A novel vector to enable multi-modal strategies for cancer therapies.
416 Adv Drug Deliv Rev. 2012;64:730–738.
417 27. Mima H, Yamamoto S, Ito M, Tomoshige R, Tabata Y, Tamai K, Kaneda Y. Targeted
418 chemotherapy against intraperitoneally disseminated colon carcinoma using a cationized
419 gelatin-conjugated HVJ envelope vector. Mol Cancer Ther. 2006;5(4):1021–1028.
420 28. Zhang Q, Li Y, Shi Y, Zhang Y. HVJ envelope vector, a versatile delivery system: Its
421 development, application, and perspectives. Biochem Biophys Res Commun.
422 2008;373:345–349.
423 29. Arhel N, Kirchhoff F. Host proteins involved in HIV infection: new therapeutic targets.
424 Biochim. Biophys. Acta 2010;1802(3):313-321.
425 30. Kim CW, Chang KM. Hepatitis C virus: virology and life cycle. Clin. Mol. Hepatol.
426 2013;19(1):17-25.
427 31. Brasch M, Voets IK, Koay MS, Cornelissen JJ. Phototrigged cargo release from virus-like
428 assemblies. Faraday Discuss 2013;166:47-57.
429 32. Niikura K, Sugimura N, Musashi Y, Mikuni S, Matsuo Y, Kobayashi S, Nagakawa K,
430 Takahara S, Takeuchi C, Sawa H, Kinjo M, Ijiro K. Virus-like particles with removal
431 cyclodextrins enable glutathione-triggered drug release in cells. Mol. Biosyst. 2013;9:501-
432 507.
433

434 **Table 1. Primers used**

Name	5’-3’
Eco-bx-FLAG-hCC49scFv	CACCATGAAGATACTCCTTGCTATTGCATTAATGTTGTCAACAGTAATGTGGGTGTCAACAGACTACAAGGATGACGATGACAAGCAGGTGCAGCTGGTG
scFv-spe	CGACTAGTGGATGATATGATGATG
Spe-H1N1	AGACTAGTGAACAATGCCAAGGAGATTG
H1N1-Hind	ATAAGCTTTTAATGGTGATGATGGTG

435

FIGURE LEGENDS

Figure 1. Schematic presentation of this study. RSV gag protein and hCC49 scFV fused with the C-terminal region of hemagglutinin from influenza A (H1N1) virus (A/duck/NY/191255-59/02) were simultaneously expressed in silkworm larvae using the BmNPV bacmid system. The hCC49 scFv-displaying RSV VLPs were obtained from collected hemolymph by sucrose density gradient centrifugation. FITC or DOX was loaded into the VLPs by electroporation. Drug delivery to colon carcinoma cells (LS174T cells) was performed using FITC- or DOX-loaded hCC49 scFv-displaying RSV VLPs.

Figure 2. Expression and purification of hCC49 scFv-displaying RSV VLPs. (A) Detection of hCC49 scFv and RSV gag protein in hemolymph and fat body of silkworm larvae by western blot. Lanes 1–3 denote molecular weight, hemolymph, and fat body samples, respectively. (B) Detection of hCC49 scFv and RSV gag protein in fractions by sucrose density gradient centrifugation of concentrated RSV VLPs. Lane 1: fractions 1 & 2; lane 2: fractions 3 & 4; lane 3: fractions 5 & 6; lane 4: fractions 7 & 8; lane 5: fractions 9 & 10. Open and closed triangles denote scFv fusion protein and Gag protein, respectively.

Figure 3. Characterization of hCC49 scFv-displaying RSV VLPs. (A) Immunofluorescence microscopy of LS174T cells treated with hCC49 scFv-displaying RSV VLPs and RSV VLPs. LS174T cells were treated with hCC49 scFv-displaying RSV VLPs and immunofluorescence microscopy was performed, as described in the Materials and Methods section. The nuclei of LS174T cells were stained with DAPI. (B) Binding assay of hCC49 scFv-displaying RSV VLPs to TAG-72 using enzyme-linked immunosorbent assay (ELISA). TAG-72 was immobilized into each well of a 96-

well ELISA plate and ELISA was performed, as described in the Materials and Methods section. 1: Hemolymph of mock, 2: Hemolymph of hCC49 scFv-displaying RSV VLPs-expressing silkworms, 3: Purified hCC49 scFv-dispaying RSV VLP. * $p < 0.01$ (C) Immunoelectron microscopy of hCC49 scFv-displaying RSV VLPs. Immunoelectoron microscopy was performed using mouse monoclonal anti-DYKDDDDK tag antibody and gold nanoparticle-conjugated goat polyclonal anti-mouse IgG+IgM (H+L). (D) Analysis of each VLP size by DLS

Figure 4. Fluorescence microscopy of LS174T cells treated with FITC-loaded RSV VLPs. FITC was loaded into hCC49 scFv-displaying RSV VLPs and RSV VLPs by electroporation. LS174T cells were incubated with each of the FITC-loaded RSV VLPs. The nuclei of LS174T cells were stained with DAPI. Green fluorescence of FITC and blue fluorescence of DAPI were observed by confocal laser scanning microscope.

Figure 5. Cell viability of LS174T and HEK293 cells treated with each of the VLPs. Gag-DOX: DOX-loaded RSV VLPs, SHG-DOX: DOX-loaded hCC49 scFv-displaying RSV VLPs, Mix: mixture of hCC49 scFv-displaying RSV VLPs with DOX (1:1), VLPs: RSV VLPs. DOX10 and DOX50 denote DOC concentration of 10 and 50 μg/ml, respectively. Grey and white bars denote LS174T and HEK293 cells, respectively.

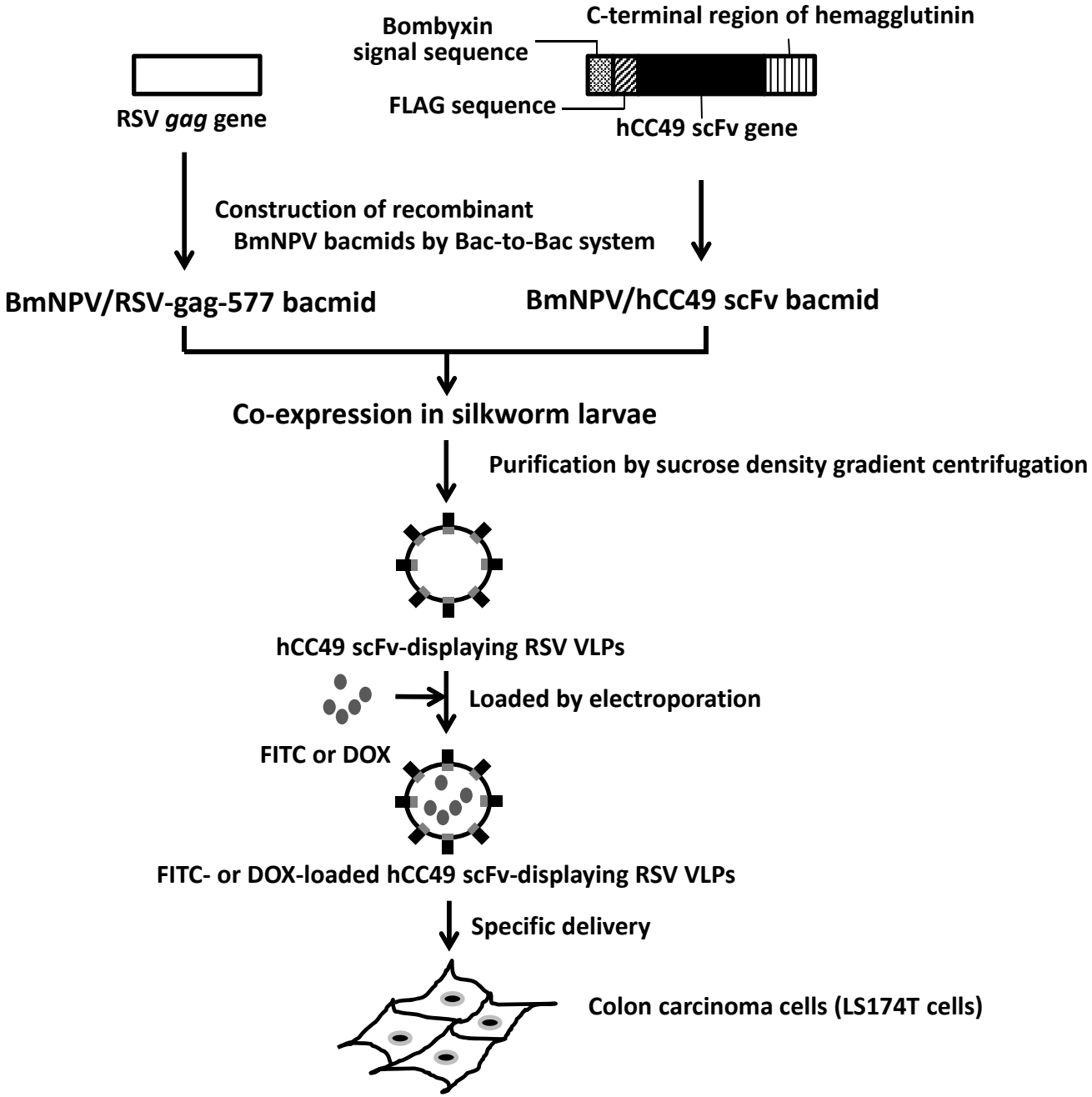
Bombyxin signal sequence
C-terminal region of hemagglutinin
FLAG sequence
hCC49 scFv gene
RSV gag gene
Construction of recombinant BmNPV bacmids by Bac-to-Bac system
BmNPV/RSV-gag-577 bacmid
BmNPV/hCC49 scFv bacmid
Co-expression in silkworm larvae
Purification by sucrose density gradient centrifugation
hCC49 scFv-displaying RSV VLPs
Loaded by electroporation
FITC or DOX
FITC- or DOX-loaded hCC49 scFv-displaying RSV VLPs
Specific delivery
Colon carcinoma cells (LS174T cells)

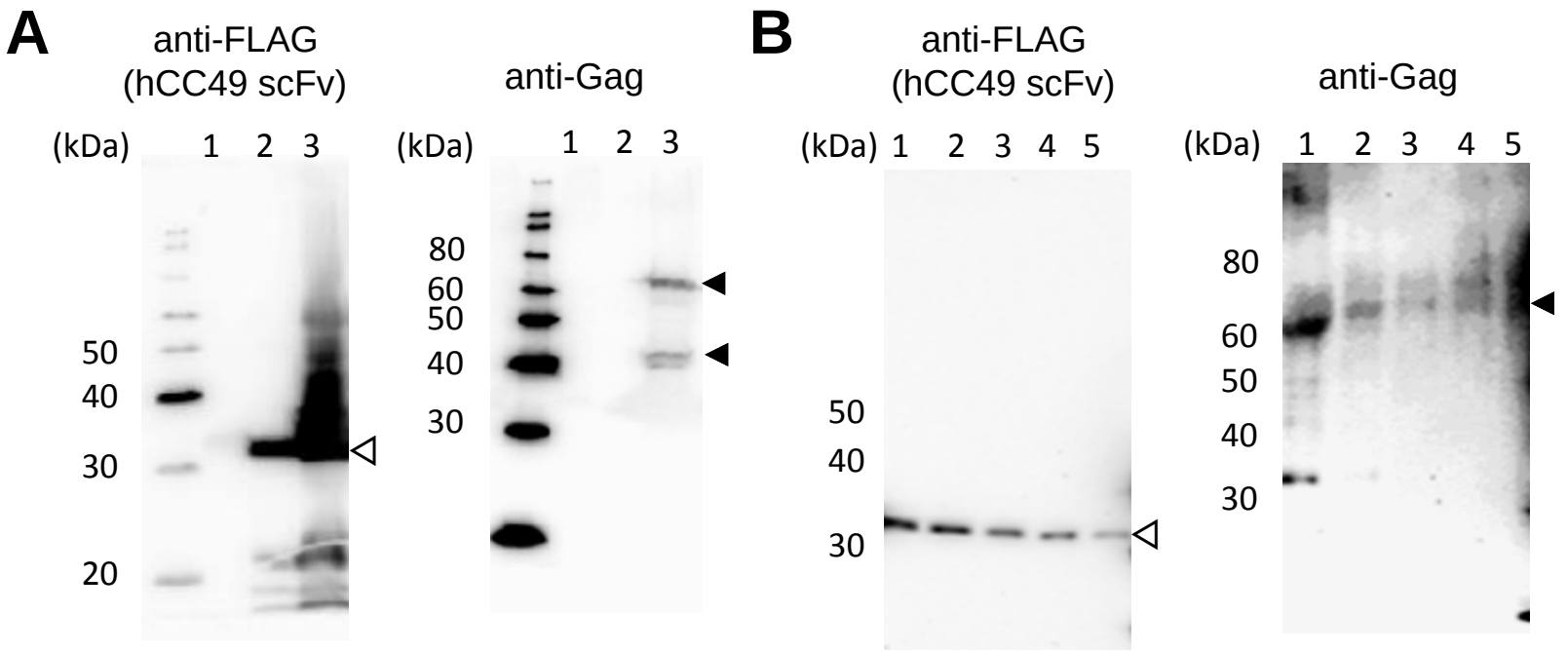
A
anti-FLAG
(hCC49 scFv)
(kDa)
1 2 3
50
40
30
20
anti-Gag
(kDa)
1 2 3
80
60
50
40
30
B
anti-FLAG
(hCC49 scFv)
(kDa)
1 2 3 4 5
50
40
30
anti-Gag
(kDa)
1 2 3 4 5
80
60
50
40
30

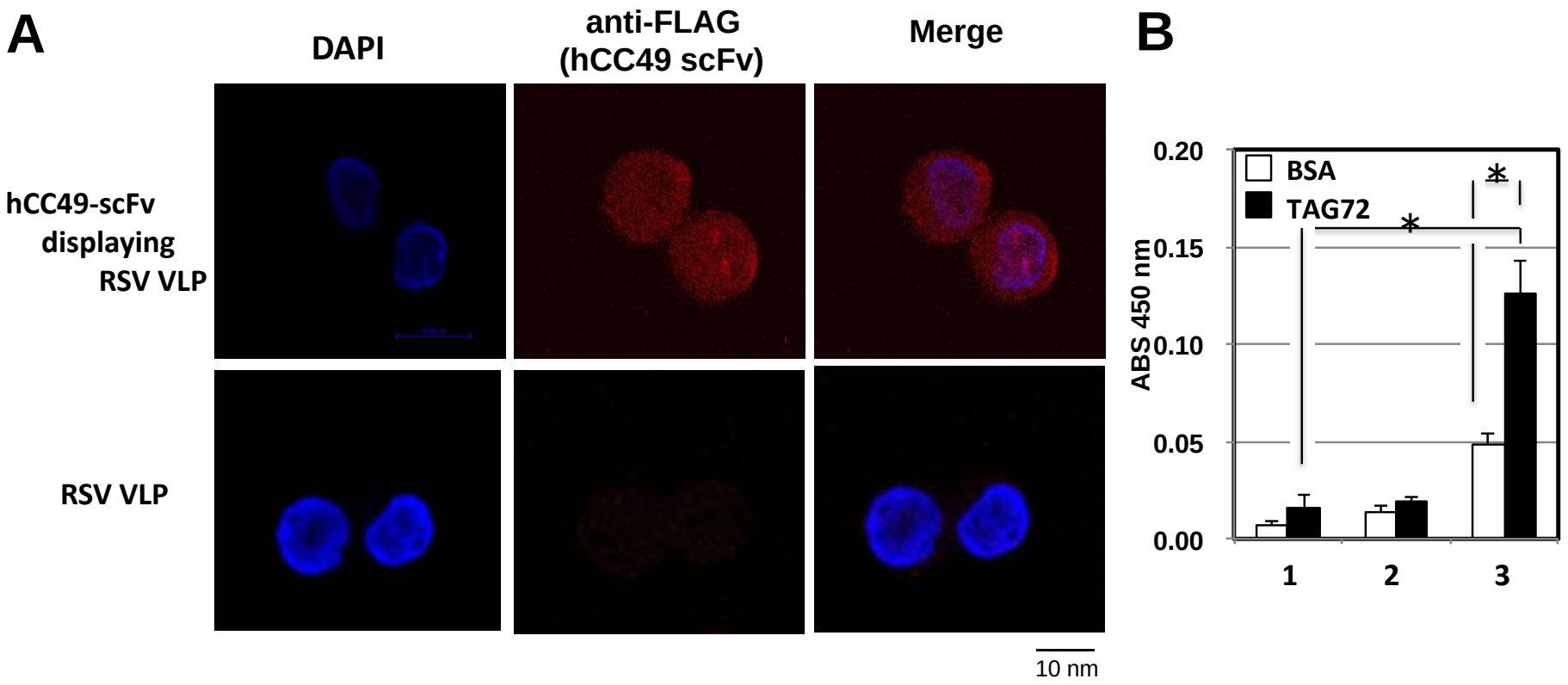
A
DAPI
anti-FLAG
(hCC49 scFv)
Merge
hCC49-scFv
displaying
RSV VLP
RSV VLP
10 nm
B
BSA
TAG72
ABS 450 nm
0.20
0.15
0.10
0.05
0.00
1
2
3
C
50 nm
D
Number (%)
25
20
15
10
5
0
0.1
1
10
100
1000
10000
Size (d.nm)
RSV VLP
hCC49 scFv
-displaying RSV VLP

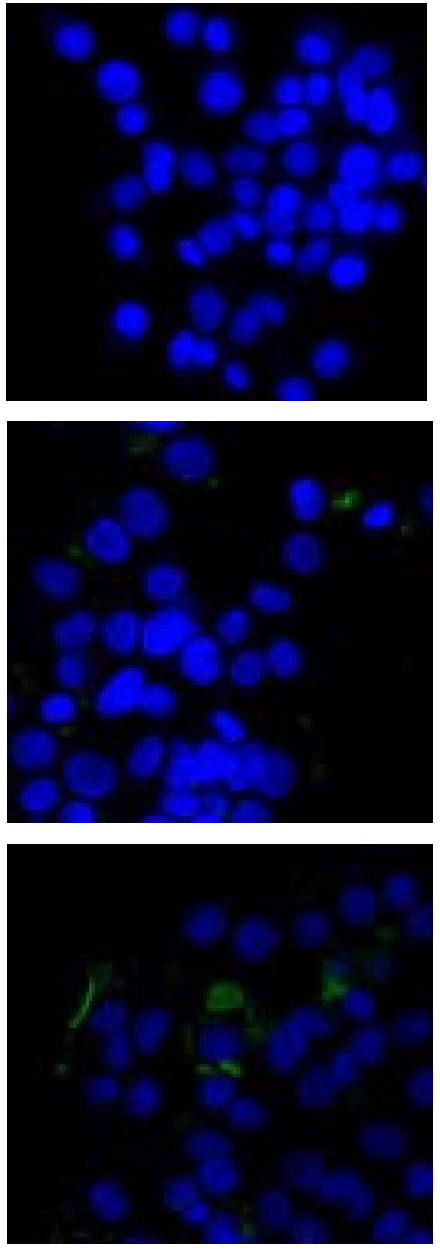
FITC
FITC-loaded
RSV VLP
FITC-loaded
HCC 49 scFv
-displaying RSV VLPs
20 μm

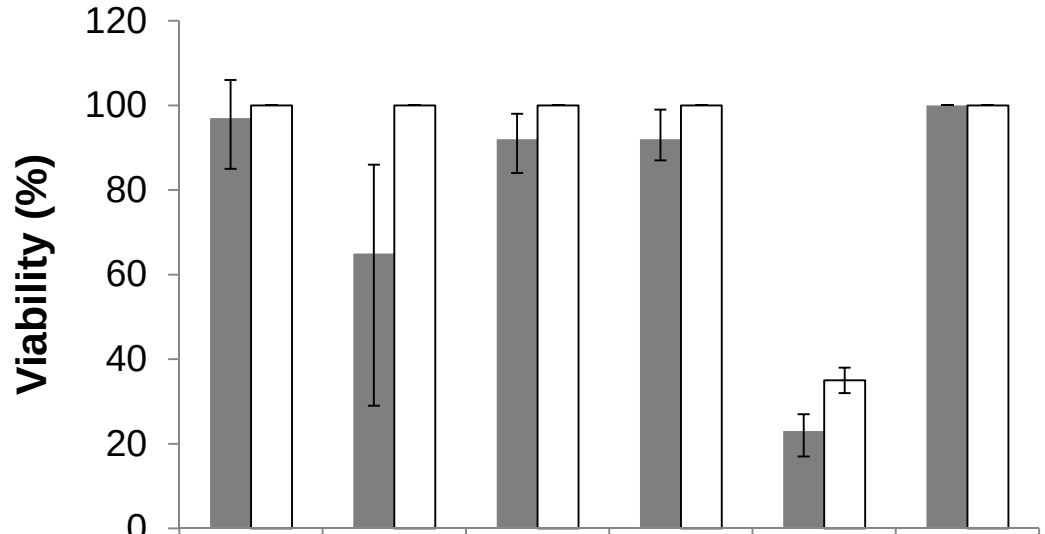

	Gag-DOX	SHG-DOX	MIX	DOX10	DOX50	VLPs
■ LS174T	97	65	92	92	23	100
□ HEK293	100	100	100	100	35	100

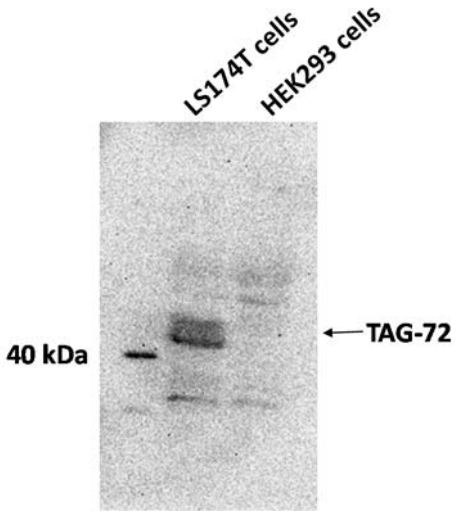

Supplementary Figure 1. TAG-72 was observed specifically by mouse anti-TAG-72 antibody (CC49, Santa Cruz Biotechnol., Cat. No. sc-20043) in LS174T cell extract (3 × 10^6 cells) at around 40 kDa. Mouse anti-TAG-72 antibody was diluted with TBST at 1:500 and HRP-conjugated anti-mouse IgG antibody was diluted with TBST at 1:15000. HEK293 cells extract (3 × 10^6 cells) was provided to confirm TAG-72 expression investigated, but molecular band of TAG-72 was not shown. It indicates that LS174T cells express TAG-72, which is targeted specifically by hCC49 scFv-displaying RSV VLPs. In the previous paper, TAG-72 was observed in LS174T cell extract at around 40 kDa, unlikely to purified TAG-72 (Cancer Res. 48, 6811-6816, 1988). Our result corresponds to the previously reported result. Specific DOX delivery to LS174T cells by hCC49 scFv displaying RSV VLPs is supported by this data and also Figure 5.